MEMS PARALLEL PLATE ACTUATORS: PULL-IN, PULL-OUT AND OTHER TRANSITIONS

Subrahmanyam Gorthi†, Atanu Mohanty† and Anindya Chatterjee*
†Supercomputer Education and Research Centre, Indian Institute of Science, Bangalore, India,
subrahmanyam.gorthi@gmail.com, amohanty@serc.iisc.ernet.in
*Mechanical Engineering, Indian Institute of Science, Bangalore, India, *anindya100@gmail.com*

ABSTRACT

The operational range of MEMS electrostatic parallel plate actuators can be extended beyond pull-in with the presence of an intermediate dielectric layer, which has a significant effect on the behavior of such actuators. Here we study the behavior of cantilever beam electrostatic actuators beyond pull-in, using a beam model. Three possible static configurations of the beam are identified over the operational voltage range. We call them floating, pinned and flat: the latter two are also called arc-type and S-type in the literature. We compute the voltage ranges over which the three configurations can exist, and the points where transitions occur between these configurations. Voltage ranges are identified where where bi-stable and tri-stable states can exist. A classification of all possible transitions, based on the dielectric layer parameters, is presented. Dynamic stability analysis is presented for the floating and pinned configurations. For high dielectric layer thickness, discontinuous transitions between configurations disappear and the actuator has smooth predictable behavior, but at the expense of lower tunability. We suggest that variable dielectric layer thickness may be used to obtain both regularity/predictability as well as high tunability.

I. INTRODUCTION

This paper presents a study of cantilever beam MEMS electrostatic actuators beyond pull-in. The effects are studied of an intermediate dielectric layer on possible configurations of the actuator and transitions between them.

The behavior of MEMS electrostatic parallel plate actuators before pull-in is studied extensively in the literature. These actuators can be meaningfully modeled beyond pull-in with the presence of an intermediate dielectric layer between the electrodes. Many MEMS devices operate beyond pull-in, e.g., capacitive switches [1], [2], zipper varactors [3], [4], and tunable CPW resonators [5].

The cantilever beam electrostatic actuator is illustrated in Fig. 1. It has three possible configurations in the entire operational range. These configurations differ in the boundary conditions at the free end of the cantilever beam and are as follows.

1) ***Floating Configuration:*** The cantilever beam has no contact with the dielectric layer and is illustrated in Fig. 3(a). The bending moment and shear force at the free end are zero.
2) ***Pinned Configuration:*** The free end of the cantilever beam touches the dielectric layer but is free to pivot about the contact point and is illustrated in Fig. 3(b). The deflection (measured from the dielectric layer) and the bending moment are zero at the touching end.
3) ***Flat Configuration:*** A non-zero length of the beam is in contact with the dielectric layer, as illustrated in Fig. 3(c). The contact length of the cantilever beam varies with the applied voltage. Deflection measured

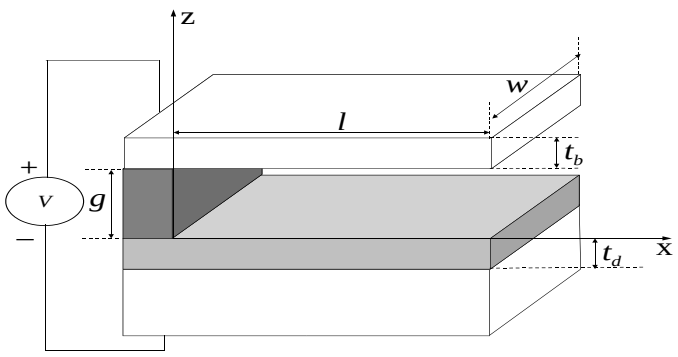

Fig. 1: Schematic view of the cantilever beam electrostatic actuator.

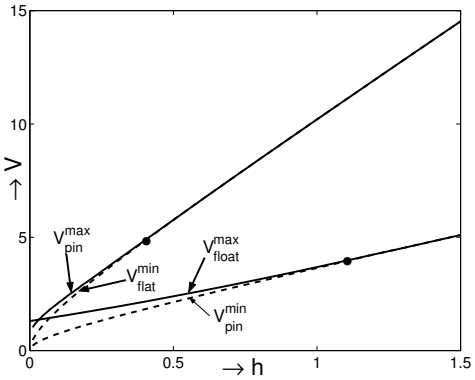

Fig. 2: V limits for different configurations.

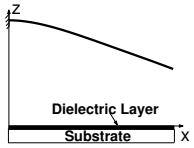

(a) Floating configuration.

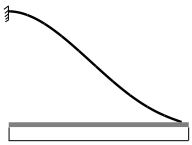

(b) Pinned configuration.

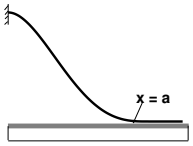

(c) Flat configuration.

Fig. 3: Possible static configurations of the cantilever beam actuator. (The scale in the vertical direction is exaggerated.)

from the dielectric layer, slope and moment are zero at the point separating the contact and the non-contact regions of the cantilever. The point is denoted by $x = a$ in Fig. 3(c). The shear force is nonzero at this point. Note that, unlike the previous two configurations, the non-contacting region is not known in advance.

II. MODELING AND SIMULATIONS

The non-contact portion of the beam for all the three configurations is governed by the same equation although the boundary conditions differ. The 1-D equation governing the mechanical deformation of an Euler-Bernoulli beam, neglecting the fringing field, is

$$E\,I\,\frac{\partial^4 z}{\partial x^4} + \rho\,\frac{\partial^2 z}{\partial t^2} = -\frac{\epsilon_0\,w\,V^2}{2\left(z + \dfrac{t_d}{\epsilon_r}\right)^2}. \tag{1}$$

The variables x and z in the above equations denote the position along the length and the lateral deflection of the beam respectively; t is time; E is Young's modulus of the material; I is moment of inertia of the beam cross-section; ρ is mass per unit length of the beam; ϵ_0 and ϵ_r are permittivity of free space and dielectric constant respectively. The other parameters are marked in Fig. 1. Effects like step-ups, stress-stiffening and softened contact surfaces are not included in this model.

The length quantities x and z (refer to Fig. 1) are normalized with respect to the length and zero bias height of the beam. Time t is normalized with respect to a constant $T = \sqrt{\frac{\rho\,l^4}{E\,I}}$, defined in such a way that the coefficient of the term containing the time derivative in Eq. 1 becomes unity. Two other non-dimensional

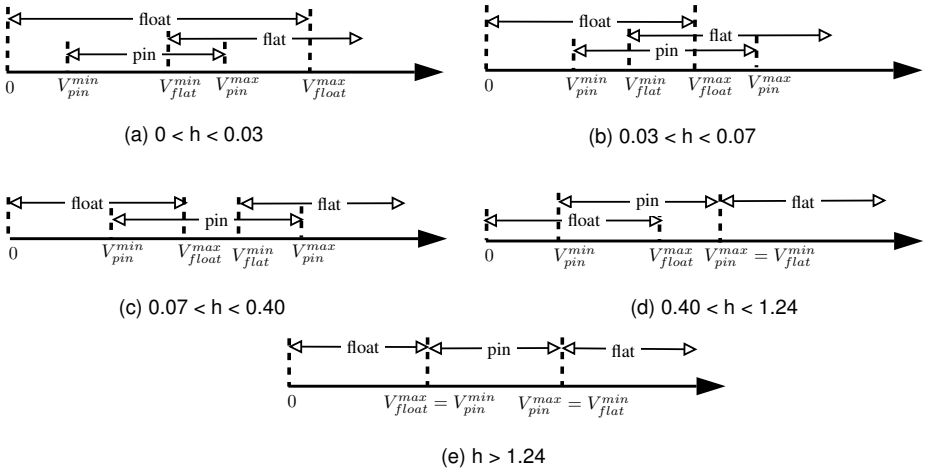

Fig. 4: Classification of possible transitions based on the numerical results of Fig. **??**.

quantities are defined and are: $\hat{V} = \sqrt{\dfrac{\epsilon_0 w\, l^4}{2\, E\, I\, g^3}}\, V$ and $h = \dfrac{t_d}{g\, \epsilon_r}$. The governing equation becomes

$$\frac{\partial^4 \hat{z}}{\partial \hat{x}^4} + \frac{\partial^2 \hat{z}}{\partial \hat{t}^2} = -\frac{\hat{V}^2}{(\hat{z}+h)^2}. \tag{2}$$

For static analysis, there is no time dependence and the equation reduces to

$$\frac{d^4 \hat{z}}{d\hat{x}^4} = -\frac{\hat{V}^2}{(\hat{z}+h)^2}. \tag{3}$$

The hats in the normalized equation are now dropped for convenience. Equation 3 constitutes a nonlinear boundary value problem for the floating, pinned configurations, and a nonlinear free boundary problem for the flat configuration. They are solved using a finite difference scheme through an iterative procedure. The system can have multiple solutions for a given V within the same configuration. All the physically feasible solutions are obtained by varying the initial guess made in the iterative procedure. The following section presents the effects of dielectric layer.

III. Effects of the Dielectric Layer

The governing Eq. 3 has only two parameters V and h. h is proportional to the dielectric thickness for a given zero bias height and dielectric constant. Similarly, V is proportional to the applied voltage. We study solutions for fixed h and varying V, for a range of values of h.

The lower voltage limit for the floating configuration is trivially zero. There is no upper voltage limit for the flat configuration since the non-contacting length approaches zero as $V \to \infty$. The other V limits vary with the h value and are computed by solving Eq. 3 for the corresponding boundary conditions and the results are shown in Fig. 2. Possible transitions between configurations are shown in Fig. 4, based on Fig. 2. There may be two or even three stable configurations at a given V. As V is changed back and forth so that transitions occur between states, therefore, there can be hysteresis in the actuator's behavior. Note that there is no such bi-stability for $h > 1.24$; and that there is *tri*-stability for $h < 0.07$.

The existence of tri-stable states has not previously been noted for such actuators in the literature.

A. Transitions

Four transitions are identified, as suggested by Fig. 4.

1) ***Pull-In****:* Pull-in occurs when the floating configuration solution disappears, as discussed earlier. The jump in the height at the free end of the beam at the point of transition results from a turning point bifurcation, as discussed later. It is interesting to note that for $h < 0.03$ (Fig. 4(a)), the transition from floating has to be to the flat configuration. For $0.03 < h < 0.07$ (Fig. 4(b)), the transition can be to either the pinned or the flat configuration, and only a full nonlinear dynamic analysis (not attempted here) can resolve which configuration is reached immediately after pull-in. For $h > 0.07$, the transition has to be to the pinned configuration. Upon increasing the voltage, regardless of h, any pinned configuration will transition to a flat configuration.

2) ***Pull-Down****:* The transition from the pinned to the flat configuration is referred to here as *pull-down*. The pinned configuration has a nonzero slope at the beam's end point, while the flat configuration has zero slope. As is the case for pull-in, a discontinuous transition from pinned to flat occurs due to a turning point bifurcation, as discussed later. As V is increased from V_{pin}^{max}, the magnitude of the slope at the touching end point decreases faster and faster, until the curve turns around (not shown here; see discussion later) and the pinned solution disappears.

3) ***Pull-Up****:* Starting in the flat configuration, a transition is possible to a pinned configuration. Here, we refer to such a transition as pull-up. Again, for $h > 0.4$, pull-up is continuous (Fig. 4). In addition, for $h < 0.07$, it is not clear without nonlinear dynamics analysis (not conducted here) whether the transition at V_{flat}^{min} occurs to the pinned or the floating configuration. Note that any pinned configuration must eventually transition to the floating configuration as V is decreased.

4) ***Pull-out****:* Finally, the transition from either pinned or flat to floating is called pull-out. Note that, as is widely observed in experiments, pull-out does not in general occur at the same voltage as pull-in; however, for large enough h, it does. This consistency in physical behavior may be useful in applications.

IV. Dynamic Stability of Equilibrium Solutions

The dynamic stability of an equilibrium solution can be determined by considering small variations of that solution, and is governed by an eigenvalue problem.

Let z_{eq} be an equilibrium solution. Then

$$\frac{\partial^4 z_{eq}}{\partial x^4} = -\frac{V^2}{(z_{eq}+h)^2} \tag{4}$$

Let ξ be a small perturbation to z_{eq}. Putting

$$z = z_{eq} + \xi \tag{5}$$

in Eq. 2,

$$\frac{\partial^4 (z_{eq}+\xi)}{\partial x^4} + \frac{\partial^2 (z_{eq}+\xi)}{\partial t^2} = -\frac{V^2}{(z_{eq}+\xi+h)^2}.$$

This system is linearized for a small value of ξ and then, discretized using modal expansion method along the lines of [6]. The eigen values of the resulting system are computed which determine the dynamic stability of the equilibrium solutions. If all the eigen values are real and negative, the solution is stable. A positive eigen value implies instability. At the stability boundary, one eigen value will be zero (a degenerate case). Figures 5(a) and 5(b) show the results of stability analysis for the floating and pinned configurations respectively. Each point on each curve represents an equilibrium solution (floating or pinned). Solid lines indicate stable, and dashed lines unstable solutions. Where the two branches coalesce in a turning point, the solution is borderline unstable by linear analysis. The value of V at the turning point represents pull-in and pull-down in the floating and pinned configurations respectively.

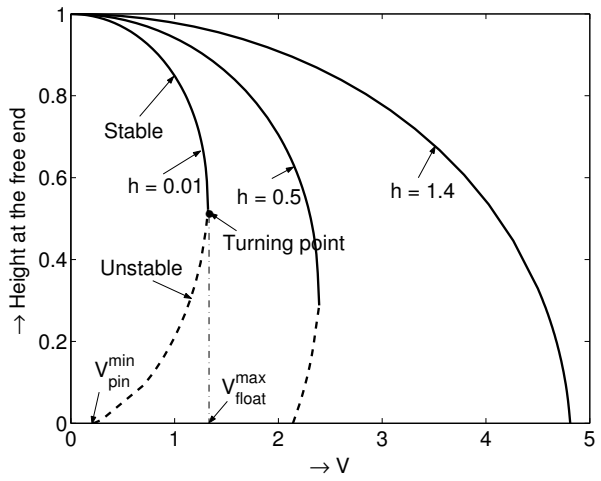

(a) Floating configuration: Variation of height at the free end of the beam with the applied voltage.

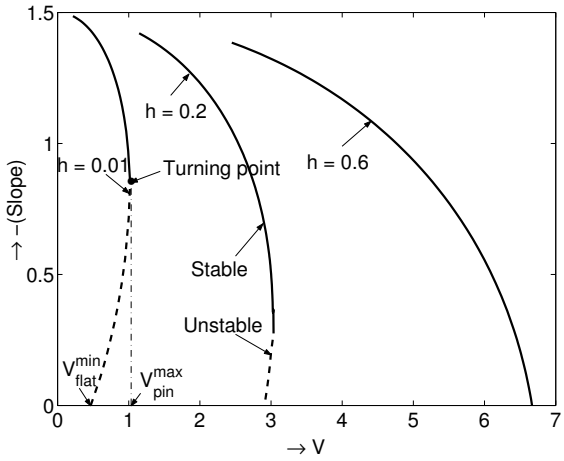

(b) Pinned configuration: Variation of slope at the pinned end with applied the applied voltage.

Fig. 5: Stability analysis of equilibrium solutions of the normalized governing equation

V. CONCLUSIONS

Cantilever beam electrostatic actuators with an intermediate dielectric layer have been analyzed in detail over the entire operational range using a beam model. Three qualitatively different configurations, here called floating, pinned and flat, have been identified and studied. Transitions from and to the floating configuration (pull-in and pull-out) and transitions from pinned to flat (pull-down) and flat to pinned (pull-up) have been identified as well. Dynamic stability analyses have complemented the study of these configurations and transitions. Both the bi-stable and tri-stable states have been found.

Higher dielectric thickness gives more regular and predictable behavior, at the cost of lower overall tunability in device characteristics. Hence, in future work, variable dielectric thickness may be studied with a view to obtaining desired behavior beyond pull-in. In particular, we suggest that a low dielectric thickness over most of the beam, smoothly increasing to a significantly larger value near the free end, may give both more regular and reversible behavior as well as higher tunability.

REFERENCES

[1] C. Goldsmith, J. Randall, S. Eshelman, T. H. Lin, D. Denniston, S. Chen, and B. Norvell, "Characteristics of micromachined switches at microwave frequencies," in *IEEE MTT-S International Microwave Symposium Digest*, vol. 2, San Francisco, June 1996, pp. 1141–1144.

[2] J. B. Muldavin and G. M. Rebeiz, "High-isolation CPW MEMS shunt switches – Part 1: Modeling," *IEEE Trans. Microwave Theory Tech.*, vol. 48, no. 6, pp. 1045 – 1052, June 2000.

[3] E. S. Hung and S. D. Senturia, "Tunable capacitors with programmable capacitance-voltage characteristic," in *Solid-State Sensors and Actuators Workshop*, June 1998, pp. 292–295.

[4] G. V. Ionis, A. Dec, and K. Suyama, "A zipper-action differential micro-mechanical tunable capacitor," in *Proceedings of MEMS Conference*, Aug., pp. 24–26.

[5] T. Ketterl, T. Weller, and D. Fries, "A micromachined tunable CPW resonator," in *IEEE MTT-S International Microwave Symposium Digest*, vol. 1, Phoenix, AZ, May 2001, pp. 345–348.

[6] Y. C. Hu, C. M. Chang, and S. C. Haung, "Some design considerations on the electrostatically actuated microstructures," *Sensors Actuators A*, vol. 112, no. 1, pp. 155–161, Apr. 2004.